Title

A MODIFIED PEIERLS MODEL FOR THERMALLY-ACTIVATED DEFORMATION IN BODY-CENTERED-CUBIC METALS

Authors

Dorn, J.E.
Mukherjee, A.K.

Publication Date

1968-03-01

Submitted to Transactions of the AIME

UCRL-18151 Rev.
Preprint
cy. 2

A MODIFIED PEIERLS MODEL FOR THERMALLY-ACTIVATED DEFORMATION IN BODY CENTERED CUBIC METALS

J. E. Dorn and A. K. Mukherjee

April 1969

AEC Contract No. W-7405-eng-48

LAWRENCE RADIATION LABORATORY
UNIVERSITY of CALIFORNIA BERKELEY

DISCLAIMER

A MODIFIED PEIERLS MODEL FOR THERMALLY-ACTIVATED DEFORMATION IN BODY CENTERED CUBIC METALS

J. E. Dorn and A. K. Mukherjee

Inorganic Materials Research Division, Lawrence Radiation Laboratory, and Department of Materials Science, College of Engineering, University of California, Berkeley, California and Department of Mechanical Engineering, College of Engineering, University of California, Davis, California.

April 1969

ABSTRACT

A modified Peierls model is presented for the rationalization of the asymmetric plastic behavior of single crystals of bcc metals. The model assumes that the asymmetry of slip arises from a tendency toward asymmetric splitting of the a/2⟨111⟩ screw dislocation. The approach differs from former theories, however, insofar as it assumes that the splitting is so minor that only the core energy is modified and that no real partial dislocations exist. As a consequence, the concepts of a line energy of a partial dislocation, interacting between partial dislocations, constriction energies and stacking fault energies are not invoked. Instead the present analysis is based on a specialization of the Peierls mechanism which assumes an asymmetric dislocation core which is modified by the effective stress and permits cross slip.

The theoretical predictions on the stress-temperature-strain rate and orientation relationship agree qualitatively with the limited experimental data that are currently available. Additional experimental work over wider ranges of conditions is suggested to provide more complete evaluation of the possible validity of this theory.

I. INTRODUCTION

Recent experimental investigations on the low-temperature thermally-activated deformation of body-centered cubic metals have confirmed the existence of several unique orientation effects. These will be described with the aid of the standard sterographic projection shown in Fig. 1. If slip were determined exclusively by crystal symmetry, the deformation characteristics would be symmetrical about $\chi_1' = 0$ and independent of whether the specimen were subjected to a tension or a compression stress, regardless of what combinations of slip planes might be operative. Experiments, however, reveal that neither of these symmetry-based predictions are valid. A schematic representation of the commonly observed asymmetry of both the yield stress and the plane of slip is shown in Fig. 2. A reversal of the direction of stressing results in an inversion of the asymmetric behavior.

1. Asymmetry of Yielding:

A detailed investigation on the asymmetric yielding in an Fe - 2.7% Si alloy was reported by Taoka, Takeuchi and Furubayashi[1]. Similar trends have been observed by Keh and Nakada on Fe[2], Stein on Mo[3], Bowen, Christian and Taylor[4] on Nb, Sherwood, Guiu, Kim and Pratt[5] on Ta, Nb and Mo. The degree of asymmetry not only depends on the atomic number and alloying but, in all cases that have been examined, it also increases with a decrease in the test temperature.

2. Asymmetry of the Slip Plane:

Asymmetric $\psi_1 - \chi_1'$ curves of the type shown in Fig. 2 have been found for several Fe- Si alloys [6,7,8,1] and Nb[4]. There is general agreement that near $\chi_1' = 30^\circ$ slip occurs by the [111] $(\bar{2}11)$ mode so that $\psi_1 = 30^\circ$. As χ_1' decreases it appears that [111] $(\bar{2}11)$ to [111] $(\bar{1}01)$ cross slip takes place leading to slip band traces on intermediate planes. And as χ_1' approaches 0°, sharp slip bands of the [111] $(\bar{1}01)$ mode result giving $\psi_1' = 0$. Some investigators [6,7,8] have suggested that after χ_1' becomes somewhat negative cross slip between the [111] $(\bar{1}01)$ and [111] $(\bar{1}\bar{1}2)$ slip modes takes place and finally at values of χ_1' approaching -30° slip occurs exclusively by the [111] $(\bar{1}\bar{1}2)$ mode. In contrast other investigators[1,4] have reported that as χ_1' decreases somewhat below 0°, the [111] $(\bar{1}01)$ mode is replaced by the $[\bar{1}11]$ $(1\bar{1}2)$ mode. There is some evidence[4] that $[\bar{1}11]$ (101) cross slip might also take place in this range.

The current somewhat unsatisfactory state of knowledge concerning operative slip systems in bcc metals has been reviewed recently by Bowen et. al[4] and by Kroupa et. al[8]. It is increasingly evident, however, that the asymmetry of the yield stress and the asymmetry of the operative slip systems have a common origin.

3. Asymmetry of Stressing:

Taoka, et. al[1], Sestak and Zarubova[6], Sestak, Zarubova and Sladek[7] and Vitek, et. al.[9] have demonstrated, that in Fe - Si alloys, the asymmetries for the yield stress and the slip systems are inverted when the sign of the stress is changed from tension to compression. They suggest the equivalence of $(\bar{2}11)$ [111] with $(\bar{1}\bar{1}2)$ $[\bar{1}\bar{1}\bar{1}]$ difficult slip and also the equivalence of $(\bar{2}11)$ $[\bar{1}\bar{1}\bar{1}]$ with $(\bar{1}\bar{1}2)$ [111] easy slip. This indicates that slip is difficult when the atoms move in the antitwinning direction, e.g., [111] slip on the $(\bar{2}11)$ plane under tension, and easy when the atoms move in the twinning direction, e.g., [111] slip on the $(\bar{1}\bar{1}2)$ plane under tension [10,11].

4. Role of Screw Dislocations:

Low and Guard[12] (Fe - Si), Low and Turkalo[13] (Fe - Si), Keh[14] (Fe), Keh and Nakada[15] (Fe), Taylor and Christian [16] (Nb) and Bowen et. al.[4] (Nb) found that most a/2 [111] dislocations lie in screw orientation following low temperature deformation. This preference, however, is somewhat reduced when the specimens are deformed at higher temperatures. These observations suggest that screw dislocations encounter higher barriers to their motion than edge dislocations and furthermore, they can be thermally activated over such barriers.

Dislocations in screw orientation exhibit the unique possibility of lowering their energy by splitting so as to dissociate into partial dislocations lying in several slip planes coincident with their zone axis.

Kroupa[17] described the symmetrical splitting of the a/2 [111] screw dislocation into four partial dislocations lying on three {110} planes. Hirsch[18] suggested the possible symmetrical splitting of screw dislocations into three partial dislocations on the {112} planes. Later Sleeswyk[19] illustrated that a lower energy splitting could take place on two {112} planes. In addition, various sequential and composite combinations of splitting[4,8,11] have been considered, several of which were described recently by Duesbery and Hirsch[20].

Escaig, Fontaine, and Friedel,[21] Kroupa and Vitek[8] and more recently Duesbery and Hirsch[20] have attempted to rationalize the low-temperature deformation of bcc metals in terms of thermally-activated cross slip of split screw dislocations. These models have proven to be somewhat interesting insofar as they can, at least qualitatively, account for the asymmetric plastic behavior of bcc metals. In general, however, they seem to suggest more rapid increases in the yield strength with decreasing temperature than is obtained experimentally. Minor objections to these models arise as a result of questionable special details of kinds of splittings that have been somewhat arbitrarily assumed. A major objection to all of these proposed cross-slip models, however, arises as a result of their internal inconsistencies. In order to achieve even nominal agreement with the experimental facts, it must be assumed that the partial dislocations are separated from each other by at most about one Burgers vector. Under these conditions the partial dislocations cores overlap and the usual concepts of line energies, interaction energies and constrictions energies for partial dislocations plus the concept of a stacking-fault energy are no longer valid. Thus the very foundation on which these models have been erected are exposed as invalid.

Despite the recent emphasis on cross slip models, the Peierls mechanism nevertheless remains as the most attractive alternate contender for rationalizing deformation in bcc metals: 1. As shown by Conrad,[22] Dorn and Rajnak,[23] Christian and Masters,[24] and Guyot and Dorn,[25] the low temperature plastic behavior of many polycrystalline bcc metals is in excellent agreement with the requirements for a Peierls mechanism. 2. Furthermore, as shown by Lau, Ranji, Mukherjee, Thomas, and Dorn,[26] for Mo and Ta and Keh and Nakada,[15] for Fe, single crystals of bcc metals so oriented as to promote, $(\bar{1}01)$ [111] slip also give results in excellent agreement with the Peierls mechanism. Obviously, the previously formulated Peierls mechanism seems to account well for most of the facts excepting those associated with asymmetric effects.

There already exists rather definitive evidence that as the stacking-fault energy increases the cross-slip mechanism can be replaced by a Peierls mechanism. The critical observation concerns the changes in the low-temperature mechanisms for prismatic slip in Mg as a function of Li content. Ahmadieh, Mitchell, and Dorn,[27] Mitchell and Dorn,[28] and Dorn[29] have shown that, below about 8 atomic % Li, prismatic slip is controlled by the Friedel[30] mechanism for cross slip from the basal plane, on which screw dislocations dissociate into Shockley partials, onto the prism plane following costriction and recombination of the partial dislocations. Estimates based on the intersection energy (from basal slip), the constriction energy and the recombination energy (from cross slip) place the stacking-fault width in pure Mg at 4 to 8 Burgers vectors. The observed trends of the effective stress, τ^*, at various temperatures T,and of the activation volume versus τ^* relationship for prismatic slip with increasing Li content suggests that Li increases the stacking-fault energy of Mg, thus decreasing the separation of the partial dislocations on the basal plane and facilitating cross slip of screw dislocations to the prism planes. Above about 8 atomic % Li, however, the Friedel cross slip mechanism no longer applies and the data agree extremely well with the Peierls theory. The Peierls stress decreases modestly as the Li content is increased from 10 to about 12 atomic %. These observations reveal that a "true" cross-slip mechanism can change into a pseudo-Peierls mechanism when the stacking-fault energy becomes sufficiently high.

It is a thesis of this report that the stacking fault energies of many bcc metals are so high and their screw dislocations are so modestly dissociated that it is highly inappropriate to attempt to formulate their low-temperature plastic behavior in terms of the usual continuum models for cross slip. The tendency toward dissociation, however, results in a readjustment of the positions of atoms in the dislocation core with a consequent lowering of the energy of a screw dislocation. Several recent theoretical investigations[31-33] on the arrangement of atoms in the core of screw dislocations provides support for this concept. The implication is that as the screw dislocation moves from one to an adjacent row of atoms on its slip plane, the core atoms must be moved into a more planar arrangement with a consequent increase in the core energy. Consequently a Peierls-type of approach appears to be capable of describing the behavior.

Very recently Duesbery and Hirsch[20] have suggested an extension of Seeger's[34] original double-kink model to account for the thermally-activated cross slip of a dissociated screw dislocation. Their major interest concerned principally the effective stress versus temperature relationship without reference to the asymmetries. Their model, more-over is restricted to low values of the effective stress, i.e., the higher temperatures of the significant range, where the asymmetric behavior is least pronounced. The predictions of this very special model, however, illustrate the potentialities of approaching the low-temperature thermally-activated deformation of bcc metals on the basis of a Peierls-like mechanism.

It is the objective of this report to introduce a pseudo-Peierls mechanism based on modification of the line-energy normal-Peierls models[23,25,35] that takes into consideration, at least qualitatively, the asymmetry of the core of screw dislocations. It will be shown that the deductions based on this model are in reasonable agreement with most of the observed asymmetries in slip band formation and in the variations of the effective stress versus temperature relations as a function of crystal orientation.

II. THE PSEUDO-PEIERLS MECHANISM

The following discussion of the pseudo-Peierls mechanism will be based on an extension of the Dorn-Rajnak[23] approach to the Peierls process. The kink energy, U_k, can be approximated by

$$U_k = \frac{2\Gamma a}{\pi}\left(\frac{2\tau_p ab}{\pi\Gamma}\right)^{1/2} \qquad (1)$$

where $\Gamma \approx Gb^2/2$ is the dislocation line energy, G is the shear modulus of elasticity, a the spacing between the Peierls valleys, b the Burgers vector and τ_p the Peierls stress. Furthermore, the energy, U_n, that need be supplied by a thermal fluctuation in order to nucleate a pair of kinks will be taken as

$$U_n = 2U_k \quad f\left\{\frac{\tau^*}{\tau_p}\right\} \simeq \frac{4\Gamma a}{\pi}\left(\frac{2\tau_p ab}{\pi\Gamma}\right)^{1/2} \quad (1 - \tau^*/\tau_p)^{3/2} \qquad (2)$$

where τ^* is the effective resolved shear stress on the slip plane. The analytical expression adopted in Eq. 2 for U_n agrees well with that given by the Dorn-Rajnak model for a sinusoidal Peierls hill. Although other shapes of Peierls hills, e.g. the quasi-parabolic type,[25] might prove more appropriate in this analysis, it has been shown that the theoretical predictions are insensitive to modest variations in the types of hills that are assumed. The following assumptions will be made:

(1) The thermally-activated deformation of bcc metals is controlled by thermally-assisted formation of kink pairs on screw dislocations.

(2) For tensile or compression axes within the standard stereographic triangle (vide Fig. 1) only the 1/2 [111] and the 1/2 [$\bar{1}$11] screw dislocations become activatable. This arises because the resolved shear stress is too low to induce activation of other screw dislocations. Thus the analysis is not strictly valid for specimen axes at the corners of the unit triangle or along its edges since other screw dislocations induce polyslip for these special orientations. (3) Slip can take place only on planes of the form {101} and {112} that belong to the [111] and [$\bar{1}$11] zone axes. The theory can easily be modified to include slip on planes of other forms, e.g. {123}, if an when definitive evidence for the operation of such slip planes is obtained. (4) Cross slip of the 1/2 [111] screw dislocation will be assumed to take place between the ($\bar{1}$10), ($\bar{2}$11), ($\bar{1}$01), ($\bar{1}\bar{1}$2) and (0$\bar{1}$1) planes. The specimen orientation will be given by λ_1 and χ_1' shown in Fig. 1. (5) Cross slip of the 1/2 [$\bar{1}$11] screw dislocation will be assumed to take place between the (110) (211), (101), (1$\bar{1}$2) and (0$\bar{1}$1) planes. The specimen orientation relative to these slips will be designed by λ_2, χ_2', in a way consistent with the designations of λ_1 and χ_1'. Obviously λ_2 and χ_2' are not independently variable since they are fixed where λ_1 and χ_1' are established by relations $\lambda_2 \equiv \lambda_2 \{\lambda_1, \chi_1'\}$ and $\chi_2' \equiv \chi_2' \{\lambda_1, \chi_1'\}$. Since these expressions are clumsy, all equations will be written in terms of the four variables λ_1, χ_1' and λ_2, χ_2'; the correlations between these orientation variables can best be deduced directly from a sterographic projection.

When an effective tensile stress σ^* is applied in the direction λ_1, χ_1' and λ_2, χ_2', the effective resolved shear stresses on the assumed slip planes are given by

$$\tau^*_{\bar{1}10} = \sigma^* \cos\lambda_1 \sin\lambda_1 \cos(60 - \chi_1') \qquad (3a)$$

$$\tau^*_{\bar{2}11} = \sigma^* \cos\lambda_1 \sin\lambda_1 \cos(30 - \chi_1') \qquad (3b)$$

$$\tau^*_{\bar{1}01} = \sigma^* \cos\lambda_1 \sin\lambda_1 \cos\chi_1' \qquad (3c)$$

$$\tau^*_{\bar{1}\bar{1}2} = \sigma^* \cos\lambda_1 \sin\lambda_1 \cos(30 + \chi_1') \qquad (3d)$$

$$\tau^*_{0\bar{1}1} = \sigma^* \cos\lambda_1 \sin\lambda_1 \cos(60 + \chi_1') \qquad (3e)$$

$$\tau^*_{0\bar{1}1} = \sigma^* \cos\lambda_2 \sin\lambda_2 \cos(60 + \chi_2') \qquad (4a)$$

$$\tau^*_{1\bar{1}2} = \sigma^* \cos\lambda_2 \sin\lambda_2 \cos(30 + \chi_2') \qquad (4b)$$

$$\tau^*_{101} = \sigma^* \cos\lambda_2 \sin\lambda_2 \cos\chi_2' \qquad (4c)$$

$$\tau^*_{211} = \sigma^* \cos\lambda_2 \sin\lambda_2 \cos(30 - \chi_2') \qquad (4d)$$

$$\tau^*_{110} = \sigma^* \cos\lambda_2 \sin\lambda_2 \cos(60 - \chi_2') \qquad (4e)$$

The corresponding Peierls stresses for cross slip on the operative planes need to be adjusted in such a way as to account for the asymmetry of the dislocation cores. For ease of discussion these will first be written out and subsequently given their physical significance. The Peierls stress will be represented by

$$\tau_{p\bar{1}10} = P_{\bar{1}01} + A_{\bar{1}01} \sigma^* \cos \lambda_1 \sin \lambda_1 \sin 3\chi_1' \qquad (5a)$$

$$\tau_{p\bar{2}11} = P_{\bar{2}11} + A_{\bar{2}11} \sigma^* \cos \lambda_1 \sin \lambda_1 \sin 3\chi_1' \qquad (5b)$$

$$\tau_{p\bar{1}01} = P_{\bar{1}01} + A_{\bar{1}01} \sigma^* \cos \lambda_1 \sin \lambda_1 \sin 3\chi_1' \qquad (5c)$$

$$\tau_{p\bar{1}\bar{1}2} = P_{\bar{1}\bar{1}2} + A_{\bar{1}\bar{1}2} \sigma^* \cos \lambda_1 \sin \lambda_1 \sin 3\chi_1' \qquad (5d)$$

$$\tau_{p0\bar{1}1} = P_{\bar{1}01} + A_{\bar{1}01} \sigma^* \cos \lambda_1 \sin \lambda_1 \sin 3\chi_1' \qquad (5e)$$

$$\tau_{p0\bar{1}1} = P_{\bar{1}01} + A_{\bar{1}01} \sigma^* \cos \lambda_2 \sin \lambda_2 \sin 3\chi_2' \qquad (6a)$$

$$\tau_{p1\bar{1}2} = P_{\bar{1}\bar{1}2} + A_{\bar{1}\bar{1}2} \sigma^* \cos \lambda_2 \sin \lambda_2 \sin 3\chi_2' \qquad (6b)$$

$$\tau_{p101} = P_{\bar{1}01} + A_{\bar{1}01} \sigma^* \cos \lambda_2 \sin \lambda_2 \sin 3\chi_2' \qquad (6c)$$

$$\tau_{p211} = P_{\bar{2}11} + A_{\bar{2}11} \sigma^* \cos \lambda_2 \sin \lambda_2 \sin 3\chi_2' \qquad (6d)$$

$$\tau_{p110} = P_{\bar{1}01} + A_{\bar{1}01} \sigma^* \cos \lambda_2 \sin \lambda_2 \sin 3\chi_2' \qquad (6e)$$

where the A's represent asymmetry factors that account for modifications of the Peierls stress due to atomic displacements in the dislocation core as a result of the applied stress.

As suggested by Hirth and Lothe[10] the component of the Peierls stress $P_{\bar{2}11}$, obtained when the atoms are moved in the antitwinning direction, might be expected to exceed $P_{\bar{1}\bar{1}2}$ which applies when the atom motion is in the twinning direction. On the other hand, the component of the Peierls stress $P_{\bar{1}01}$ is expected to be the same for all planes of the form $(\bar{1}01)$ as assumed in Eqs. 5 and 6.

The asymmetrical components of the Peierls stress have a much more subtle origin. They are based on the concept that the asymmetrical arrangement of the atoms in the core of the dislocation is perturbed by the applied stress. To a first approximation the perturbation is expected to be linear with a resolved shear stress. For positive values of χ_1', vide Fig. 1, the perturbation will move the atoms toward the more difficulty activated arrangement whereas the opposite takes place for negative values of χ_1'. Although current knowledge regarding dislocation cores is inadequate to deal accurately in an analytical way with this hypothesis, it is expected that if these effects are not too large they should depend on sin $3\chi'$. This dependence is suggested by the three-fold symmetry axis that should apply to screw dislocations in the $\langle 111 \rangle$ directions. Since Eqs. 5 and 6 are not algebraic they need be restated in terms of symmetry and twinning directions upon reversal of the stress from tension to compression. When this is done they will also account for the observed inversions in the asymmetry effects.

Because our information on dislocation cores and how they are affected by applied stresses is so naive, a rigorous development of the asymmetric behavior cannot yet be given. Consequently, the justification for the suggested relationships given in Eqs. 5 and 6 can only be established a posteriori in terms of how accurately predictions based on these assumptions agree with the experimental facts. Therefore, their justification will be demonstrated later.

According to the approximations by Guyot and Dorn[25], the frequencies of activation of cross slip on a single (h k ℓ) plane of the [111] and [$\bar{1}$11] zones respectively are

$$\nu_{hk\ell 1} = \frac{\nu_o \; L_1 b^2 \tau_{phk\ell 1}}{\pi^2 \; a_{hk\ell} \Gamma} \quad e^{\frac{-U_{hk\ell 1}}{kT}} \tag{7a}$$

$$\nu_{hk\ell \bar{1}} = \frac{\nu_o \; L_{\bar{1}} b^2 \tau_{phk\ell \bar{1}}}{\pi^2 \; a_{hk\ell} \Gamma} \quad e^{\frac{-U_{hk\ell \bar{1}}}{kT}} \tag{7b}$$

where ν_o is the Debye frequency, L is the average length of a dislocation that might be swept out by a pair of kinks following their nucleation, Γ is the dislocation line energy, $a_{hk\ell}$ is the distance between parallel rows of atoms on the (hkℓ) plane and kT has its usual meaning of the Boltzmann constant times the absolute temperature. The subscripts on τ_p and U refer to the cross slip. The frequency of activation for cross slip of the $\frac{1}{2}$ [111] screw dislocation is independent of that of the $\frac{1}{2}$ [$\bar{1}$11] screw dislocation. On the other hand the frequency of activation of either of these dislocations on one of the possible cross slip plane is mutually exclusive of cross slip on any other of possible cross slip plane per any one event. Consequently when screw dislocations cross slip the relative probabilities of such cross slip is directly proportional to the frequencies given in Eq. 7. On this basis, the actual frequencies for cross slip are given by

$$\nu^*_{hk\ell 1} = \frac{\nu^2_{hk\ell 1}}{\nu_{\bar{1}101} + \nu_{\bar{2}111} + \nu_{\bar{1}011} + \nu_{\bar{1}\bar{1}21} + \nu_{0\bar{1}11}} \tag{8a}$$

$$\nu^*_{hk\ell\bar{1}} = \frac{\nu^2_{hk\ell\bar{1}}}{\nu_{0\bar{1}1\bar{1}} + \nu_{1\bar{1}2\bar{1}} + \nu_{101\bar{1}} + \nu_{211\bar{1}} + \nu_{110\bar{1}}} \qquad (8b)$$

Thus, paralleling the arguments presented by Dorn and Rajnak[23], the shear strain rates on any plane of the two designated zones are given by

$$\dot{\varepsilon}_{hk\ell 1} = \rho_1 b \quad a_{hk\ell}\ \nu^*_{hk\ell 1} \qquad (9a)$$

$$\dot{\varepsilon}_{hk\ell 1} = \rho_{\bar{1}} b \quad a_{hk\ell}\ \nu^*_{hk\ell\bar{1}} \qquad (9b)$$

where ρ_1 and $\rho_{\bar{1}}$ refer to the densities of the screw dislocations in these zones. In summary the total tensile strain rate, $\dot{\varepsilon}$, obtained by the tensor summation of all shear strain rates is given by

$$\begin{aligned}\dot{\varepsilon} &= \cos\lambda_1 \sin\lambda_1 \{\dot{\varepsilon}_{\bar{1}\bar{1}01}\cos(60-\chi_1') + \dot{\varepsilon}_{\bar{2}111}\cos(30-\chi_1') \\ &+ \dot{\varepsilon}_{\bar{1}011}\cos\chi_1' + \dot{\varepsilon}_{\bar{1}\bar{1}21}\cos(30-\chi_1') + \dot{\varepsilon}_{0\bar{1}11}\cos(60+\chi_1')\} \\ &+ \cos\lambda_2 \sin\lambda_2 \{\dot{\varepsilon}_{0\bar{1}1\bar{1}}\cos(60+\chi_2') + \dot{\varepsilon}_{1\bar{1}2\bar{1}}\cos(30+\chi_2') \\ &+ \dot{\varepsilon}_{101\bar{1}}\cos\chi_2' + \dot{\varepsilon}_{\bar{2}111}\cos(30-\chi_2') + \dot{\varepsilon}_{110\bar{1}}\cos(60-\chi_2')\end{aligned} \qquad (10)$$

The angles ψ, and ψ_2 that slip bands for the [111] and [$\bar{1}$11] zones make with the ($\bar{1}$01) and the (101) planes. respectively are readily established by vector additon to be

$$\cot\psi_1 = \frac{\frac{1}{2}\nu^*_{\bar{1}101}a_{\bar{1}10} + \frac{\sqrt{3}}{2}\nu^*_{\bar{2}111}a_{\bar{2}11} + \nu^*_{\bar{1}011}a_{\bar{1}01} + \frac{\sqrt{3}}{2}\nu^*_{\bar{1}\bar{1}21}a_{\bar{1}\bar{1}2} + \frac{1}{2}\nu^*_{0\bar{1}11}a_{0\bar{1}1}}{\frac{\sqrt{3}}{2}\nu^*_{\bar{1}101}a_{\bar{1}101} + \frac{1}{2}\nu^*_{\bar{2}111}a_{\bar{2}11} - \frac{1}{2}\nu^*_{\bar{1}\bar{1}21}a_{\bar{1}\bar{1}2} - \frac{\sqrt{3}}{2}\nu^*_{0\bar{1}11}a_{01\bar{1}}} \qquad (11a)$$

$$\cot\psi_2 = \frac{\frac{1}{2}\nu^*_{0\bar{1}1\bar{1}}a_{0\bar{1}1} + \frac{\sqrt{3}}{2}\nu^*_{1\bar{1}2\bar{1}}a_{1\bar{1}2} + \nu^*_{101\bar{1}}a_{101} + \frac{\sqrt{3}}{2}\nu^*_{211\bar{1}}a_{211} + \frac{1}{2}\nu^*_{110\bar{1}}a_{110}}{\frac{\sqrt{3}}{2}\nu^*_{0\bar{1}1\bar{1}}a_{0\bar{1}1} - \frac{1}{2}\nu^*_{1\bar{1}2\bar{1}}a_{1\bar{1}2} + \frac{1}{2}\nu^*_{211\bar{1}}a_{211} + \frac{\sqrt{3}}{2}\nu^*_{110\bar{1}}a_{110}} \qquad (11b)$$

III. DISCUSSION

Most of the data now available on the low-temperature deformation of bcc metals were gathered principally to provide a general perspective of the trends. Consequently no one study has yet covered the range of conditions and the type of tests needed to provide a complete check on the preceding formulation of the pseudo-Peierls mechanism. It is nevertheless appropriate, to illustrate some expected trends for simple examples and to correlate some of the current but limited data with the theoretical predictions.

A. Asymmetric Slip in Mo.

Body centered cubic metals invariably slip by the $(\bar{1}01)$ [111] mode for the orientation $\lambda_1 = 45^\circ$ and $\chi_1' = 0^\circ$. Here the σ^* - T data agree well over the low temperature range with predictions based on the Peierls mechanism. Asymmetric effects begin to enter as χ' deviates from 0°. For some metals, e.g. Nb, these effects are very mild whereas for other metals, e.g. Mo, the asymmetric behavior is interestingly pronounced.

For Mo the region over which the $(\bar{1}01)$ [111] mode of slip prevails extends from slightly negative values of χ' up to values of χ' that approaches $\approx 30^\circ$. Only minor amounts of the $(\bar{2}11)$ [111] and other modes accompany the deformation. Near $\chi' = 30^\circ$, however, some $(\bar{1}10)$ [111] slip is also expected. Over this range Eqs. 7,8,9 and 10 can be simplified to give

$$\dot{\varepsilon} = \frac{2\rho_1 L_1 b}{\pi^2 G} \cos\lambda_1 \sin\lambda_1 \nu_o$$

$$\left[\frac{\tau^2_{p\bar{1}101} \cos(60-\chi_1') \, e^{\frac{-2U_{\bar{1}101}}{kT}} + \tau^2_{p\bar{1}011} \cos\chi_1' \, e^{\frac{-2U_{\bar{1}011}}{kT}}}{\tau_{p\bar{1}101} \, e^{\frac{-U_{\bar{1}101}}{kT}} + \tau_{p\bar{1}011} \, e^{\frac{-U_{\bar{1}011}}{kT}}} \right] \tag{12}$$

The yield stress at the absolute zero is given by the condition that the smaller activation energy term in eq. 2, namely $U_{\bar{1}011}$ must also be zero. Therefore

$$P_{\bar{1}01} = \sigma^*_{oo} \cos\lambda_1 \sin\lambda_1 \tag{13}$$

where σ^*_{oo} is the yield stress at 0°K for $\chi_1' = 0$. As a consequence of eg. 5c then,

$$\sigma^*_{o\chi_1'} \cos\chi_1' = \sigma^*_{oo} + A_{\bar{1}01} \, \sigma^*_{o\chi_1'} \sin 3\chi_1' \tag{14}$$

where $\sigma^*_{o\chi_1'}$ is the yield stress at 0°K for the specimen orientation χ_1'. Thus, for present specialization, Eq. 14 permits an evaluation of the asymmetry factor $A_{\bar{1}01}$ in terms of the variation of the yield stress at the absolute zero with χ_1'. As will be emphasized later, $A_{\bar{1}01}$ for Mo appears to be about 0.4.

As shown by Eq. 12, the yield stress $\sigma^*_{T\chi_1'}$ decreases with increasing temperature and becomes zero at a critical temperature T_c. This value of T_c, of course, increases with $(\pi^2 G \, \dot{\varepsilon})/(\rho_1 \, L_1 b \cos\lambda_1 \sin\lambda_1 \nu_o)$ and also

χ_1'. For tests where these variables are held substantially constant, it will prove convenient to compare the theory with experimental data by plotting $\sigma^*_{T\chi_1'} \cos \lambda_1 \sin \lambda_1 / P_{\bar{1}01}$ as a function of T/T_c.

$$\text{Let} \quad \dot{\varepsilon} = 1.6 \times 10^{-4}/\text{sec.}$$

$$\frac{2\rho_1 L_1 b\nu_o}{\pi^2 G} = 6.6 \times 10^{-10} \text{ cm}^2/\text{dyne sec.}$$

$$\sigma^*_{oo} = 90.6 \times 10^{-8} \text{ dynes/cm}^2$$

$$A_{\bar{1}01} = 0.4$$

The solid curves in Fig. 3 refer to the theoretical predictions based on Eq. 12; the dashed curve was deduced from the $\chi_1' = 0$ data assuming that Schmid's Law applies; and the points refer to existing experimental data.

The inferences made here are most revealing. If, under usual circumstances, additional slip systems became operative as χ_1' approached 30°, the ratio of $\sigma^*_{T\chi_1'} \cos \lambda_1 \sin \lambda_1 / P_{\bar{1}01}$ would necessarily have been less than that suggested by Schmid's Law. The mere fact that this ratio is substantially greater than the expected value, reveals that the yield stress for slip on the $(\bar{1}01)$ plane increases as χ' increases, almost if not exactly, according to the dictates imposed by Eqs. 5 and 6.

The theoretical predictions agree well with the data given by Lau et al.[26] on Ta, Fe at low temperature by Keh and Nakada[2] and Fe - 2.7% Si at low temperature by Taoka et al.[1] for $\chi_1' = 0$. The more rapid increase in $\sigma^*_{T\chi_1'} \cos\lambda_1 \sin\lambda_1 / P_{\bar{1}01}$ with decreasing temperature as χ_1' approaches

$+30^{\circ}$ is also in general agreement with the experimental observations. Tests on single crystals oriented with their tensile axes at the [001] and [110] poles by Sherwood et al.[5] on Ta and Nb by Argon and Maloof[36] on W show asymmetric trends that are analogous to the above-mentioned theoretical predictions. Such data, however, cannot be analyzed here because the needed auxiliary information on the operative modes of polyslip are not available.

B. Asymmetric Slip in Fe and Fe-Si Alloys

The asymmetric slip characteristics of Fe and Fe-Si alloys appear to be intermediate between the weak effects in Nb and the strong ones in Mo. In addition, the degree of asymmetry of slip increases in Fe-Si alloys as the Si content increases above about 3%. On the other hand, Fe-Si alloys having 3% Si or less seem to exhibit about the same degree of asymmetry as Fe itself. For these reasons the asymmetric slip of Fe and Fe ∿ 3% Si alloys will be treated at one time.

There is excellent slip band evidence for the operation of the $(\bar{2}11)$ [111] mode of slip in Fe - 3% Si when $\chi_1' \simeq 30^{\circ}$; in this region cross slip might also take place by the $(\bar{1}10)$ [111] and $(\bar{1}01)$ [111] modes. Near $\chi_1' \simeq 0$ only the $(\bar{1}01)$ [111] mode of slip appears to prevail. Most of the slip band evidence supports the concept that as the specimen axis approaches the [001] pole slip takes place principally by the $(1\bar{1}2)$ $[\bar{1}11]$ mode with some cross slip to the (101) $[\bar{1}11]$ mode and minor amounts of slip by the $(\bar{1}\bar{1}2)$ [111] and $(\bar{1}01)$ [111] mode. Assuming that these are the principal slip systems, Eq. 10 can be reduced to the following specializations.

$$\dot{\epsilon} = \frac{2\rho_1 L_1 b}{\pi^2 G} \cos \lambda_1 \sin \lambda_1 \nu_o$$

$$\left\{ \frac{\tau^2_{p\bar{1}101} \cos(60-\chi_1') \, e^{\frac{-2U_{\bar{1}101}}{kT}} + \tau^2_{p\bar{2}111} \cos(30-\chi_1') \, e^{\frac{-2U_{\bar{2}111}}{kT}} + \tau^2_{p\bar{1}011} \cos \chi_1' \, e^{\frac{-2U_{\bar{1}011}}{kT}}}{\tau_{p\bar{1}101} \, e^{\frac{-U_{\bar{1}101}}{kT}} + \tau_{p\bar{2}111} e^{\frac{-U_{\bar{2}111}}{kT}} + \tau_{p\bar{1}011} \, e^{\frac{-U_{\bar{1}011}}{kT}}} \right\}$$

for $0 \leq \chi_1' \leq 30°$ (18)

and

$$\dot{\epsilon} = \frac{2\rho_1 L_1 \cos \lambda_1 \sin \lambda_1 \nu_o}{\pi^2 G}$$

$$\left\{ \frac{\tau^2_{p\bar{1}011} \cos \chi_1' \, e^{\frac{-2U_{\bar{1}011}}{kT}} + \tau^2_{p\bar{1}\bar{1}21} \cos(30+\chi_1') \, e^{\frac{-2U_{\bar{1}\bar{1}21}}{kT}}}{\tau_{p\bar{1}011} \, e^{\frac{-U_{\bar{1}011}}{kT}} + \tau_{p\bar{1}\bar{1}21} \, e^{\frac{-U_{\bar{1}\bar{1}21}}{kT}}} \right\}$$

$$+ \frac{2\rho_{\bar{1}} L_{\bar{1}} b \cos \lambda_2 \sin \lambda_2 \nu_o}{\pi^2 G}$$

$$\left\{ \frac{\tau^2_{p0\bar{1}1\bar{1}} \cos(60+\chi_2') \, e^{\frac{-2U_{0\bar{1}1\bar{1}}}{kT}} + \tau^2_{p1\bar{1}2\bar{1}} \cos(30+\chi_2') \, e^{\frac{-2U_{1\bar{1}2\bar{1}}}{kT}}}{\tau_{p0\bar{1}1\bar{1}} \, e^{\frac{-U_{0\bar{1}1\bar{1}}}{kT}} + \tau_{p1\bar{1}2\bar{1}} \, e^{\frac{-U_{1\bar{1}2\bar{1}}}{kT}}} \right. \rightarrow$$

$$\left. \overleftarrow{ + \tau^2_{p10 1\bar{1}} \cos \chi_2' \, e^{\frac{-2U_{10 1\bar{1}}}{kT}} } \atop \tau_{p10 1\bar{1}} \; e^{\frac{-U_{10 1\bar{1}}}{kT}} \right\}$$

$$\text{for } -30 \leq \chi_1' \leq 0 \qquad (19)$$

Because the existing data are so very incomplete it is necessary to make some reasonable assumptions regarding the parametric factors of Eqs. 5 and 6. The value of $P_{\bar{1}01}$ can be determined directly from the experimental data as given by Eq. 13. Let $P_{\bar{2}11} = P_{1\bar{1}\bar{2}}$ and let $A_{\bar{1}01} = 0.4$ and $A_{\bar{2}11} = A_{\bar{1}\bar{1}\bar{2}} = 0.2$. Then, as given by Eq. 5b,

$$\sigma^*_{0,30^\circ} \cos \lambda_1 \sin \lambda_1 \cos 0^\circ = P_{\bar{2}11} + 0.2\sigma^*_{0,30^\circ} \cos \lambda_1 \sin \lambda_1 \sin 90^\circ \qquad (20)$$

In this way $P_{\bar{2}11}$ can be established in terms of the yield stress at 0°K and $\chi_1' = 30^\circ$. With these selections the various yields stresses

$$\sigma^*_{o\chi_1'} \cos \lambda_1 \sin \lambda_1 \cos \chi_1' \quad \text{and} \quad \sigma^*_{o\chi_2'} \cos \lambda_2 \sin \lambda_2 \cos \chi_2'$$

for each different mode of slip at the absolute zero are shown in Fig. 4, where $\sigma^*_{oo} = 39.5\times10^8$ dynes/cm^2 and $P_{\bar{2}11} = P_{1\bar{1}2} = 20.33\times10^8$ dynes/cm^2. Only these systems having the lowest values of the resolved shear stresses will be operative at the absolute zero.

The theoretical relationship of $\sigma^*_{T\chi_1'} \cos \lambda_1 \sin \lambda_1/P_{\bar{1}01}$ with T/T_c

is shown by the solid curves in Fig. 5.

$$\text{Let}\quad \dot{\varepsilon} = 1.6 \times 10^{-4}\ \text{sec}^{-1}$$

$$\frac{2\rho_{\bar{1}}L_{\bar{1}}b\nu_o}{\pi^2 G} \simeq 4.94 \times 10^{-11}\ \text{cm}^2/\text{dyne sec.}$$

$$A_{\bar{1}01} = 0.4,\ A_{\bar{2}11} = 0.2$$

$$P_{\bar{2}11} = 20.33 \times 10^8\ \text{dynes/cm}^2,\ \sigma^*_{oo} = 39.5 \times 10^8\ \text{dynes/cm}^2$$

The calculations were based on the assumption that the preexponential term of Eq. 18 is substantially constant and that a constant tensile strain rate was applied. The datum points in Fig 5 refer to experimental results.

Introducing the same values for the variables as given earlier for figs 4 and 5, the $\psi_1 - \chi_1'$ and the $\psi_2 - \chi_2'$ relationship deduced from Eqs. 11a and 11b are shown by the solid and broken lines in Fig. 6. These theoretical deductions can be compared with the experimental datum points that are also recorded in the same figure.

Undoubtedly the major criticism that might be leveled against the pseudo-Peierls mechanism that was presented here concerns the semi-empirical rationalization of Eqs. 5 and 6 for modification of the Peierls stress. The rather striking agreement between predictions based on this theory and existing experimental data, however, suggests that although Eqs. 5 and 6 need more complete theoretical justification and perhaps future modification, the current formulation deserves some serious consideration.

IV. SUMMARY

1. A new approach for the rationalization of the asymmetric plastic behavior of single crystals of bcc metals was presented.

2. It assumes, as does some other approaches, that the asymmetry of slip arises from a tendency toward asymmetric splitting of the a/2[111] screw dislocation.

3. It differs from former theories insofar as it assumes that the splitting is so minor that only the core energy is modified, no real partial dislocations exist and, consequently, the concepts of a line energy of a partial dislocation, interactions between partial dislocations, constriction energies and stacking-fault energies are not invoked.

4. The present analysis is based on a generalization of the Peierls mechanism which assumes an asymmetric dislocation core which is modified by the effective stress and permits cross slip.

5. The theoretical predictions agree qualitatively with the limited experimental data that are now available.

6. Additional experimental data over wider ranges of conditions covering variation in slip band traces as well as flow stress as a function of temperature and orientation are required to provide more complete check on the validity of this theory.

ACKNOWLEDGEMENTS

The authors would like to express their appreciation to the United States Atomic Energy Commission for their support of this investigation through the Inorganic Materials Research Division of the Lawrence Radiation Laboratory of the University of California. A. K. Mukherjee, further would like to thank the chairman of the Department of Mechanical Engineering, University of California, Davis, California, for the computing and stenographic facilities that were made available.

REFERENCES

1. T. Taoka, S. Takeuchi and E. Furubayashi: J. Phys. Soc. Japan, 1964, vol. 19, p. 701.
2. A. S. Keh and Y. Nakada: Canada. J. Phys., 1967, vol. 45, no. 2, part 3, p. 1101.
3. D. F. Stein: Canada J. Phys., 1967, vol. 45, no. 2, part 3, p. 1063.
4. D. K. Bowen, J. W. Christian and G. Taylor: Canada. J. Phys., 1967, vol. 45, no. 2, part 3, p. 903.
5. P. J. Sherwood, F. Guiu, H. C. Kim and P. L. Pratt: Canada, J. Phys., 1967, vol. 45, no. 2, part 3, p. 1075.
6. B. Sestak and N. Zarubova: Phys. Stat. Sol., 1965, vol. 10, p. 239.
7. B. Sestak, N. Zarubova and V. Sladek: Canad. J. Phys., 1967, vol. 45, no. 2, part 3, p. 1031.
8. F. Kroupa and V. Vitek: Canad. J. Phys., 1967, vol. 45, no. 2, part 3, p. 945.
9. V. Vitek and F. Kroupa: Phys. Stat. Sol., 1966, vol. 18, p. 703.
10. J. P. Hirth and J. Lothe: Phys. Stat. Sol., 1966, vol. 15, p. 487.
11. R. A. Foxall, M. S. Duesbery, P. B. Hirsch: Canad. J. Phys., 1967, vol. 45, p. 607.
12. J. R. Low and R. W. Guard: Acta Met., 1959, vol. 7, p. 171.
13. J. R. Low and A. M. Turkalo: Acta Met., 1962, vol. 10, p. 215.
14. A. S. Keh: Phil, Mag., 1965, vol. 12, p. 9.
15. Y. Nakada and A. S. Keh: Acta Met., 1966, vol. 14, p. 961.
16. G. Taylor and J. W. Christian: Phil. Mag., 1967, vol. 15. p. 873, 893.
17. F. Kroupa: Phys. Stat. Sol., 1963, vol. 3, p. 391.

18. P. B. Hirsch: Fifth International Congress on Crystallography, Cambridge University, 1960.

19. A. W. Sleeswyk: Phil. Mag. 1963, vol. 8, P. 1467.

20. M. S. Duesbery and P. B. Hirsch: Dislocation Dynamics, (McGraw Hill, New York, 1968) p. 57.

21. B. Escaig, G. Fontain and J. Friedel: Canad. J. Phys., 1967, vol. 45, no. 2, part 2, p. 481.

22. H. Conrad: 1963, Conference on the Relation between the Structure and Mechanical Properties of Metals, Teddington (H.M.S.O., London) p. 475.

23. J. E. Dorn and S. Rajnak: Trans. TMS-AIME, 1964, vol. 230, p. 1052.

24. J. W. Christian and B. C. Masters: Proc. Roy. Soc. (London), 1964, Ser. A. vol. 281, p. 223.

25. P. Guyot and J. E. Dorn: Canada. J. Phys,. 1967, vol. 45, no. 2, part 3, p. 983.

26. S. S. Lau, S. Ranji, A. K. Mukherjee, G. Thomas and J. E. Dorn: Acta Met., 1967, vol. 15, p. 237.

27. A. Ahmadieh, J. Mitchell and J. E. Dorn: Trans. TMS-AIME, 1965, vol. 233, p. 1130.

28. J. E. Dorn and J. Mitchell: High Strength Materials, (John Wiley, New York, 1965), p. 510.

29. J. E. Dorn: 1967, Dislocation Dynamics, (McGraw Hill, New York, 1968) p. 27.

30. J. Friedel: Dislocations, Pergamon Press, Oxford, 1964, p. 264.

31. R. Chang: Phil. Mag., 1967, vol. 16, p. 1021.

32. R. Bullough and R. C. Perrin: Dislocation Dynamics, (McGraw Hill, New York, 1968) p. 175.

33. H. Suzuki: Dislocation Dynamics, (McGraw Hill, New York, 1968) p. 679.

34. A. Seeger: Phil. Mag., 1956, vol. 1, p. 651.

35. V. Celli, M. Kabler, T. Ninomiya and R. Thomson: Phy. Rev., 1963, vol. 131, p. 58.

36. A. S. Argon and S. R. Maloof: Acta Met., 1966, vol. 14, p. 1449.

LIST OF FIGURE CAPTIONS

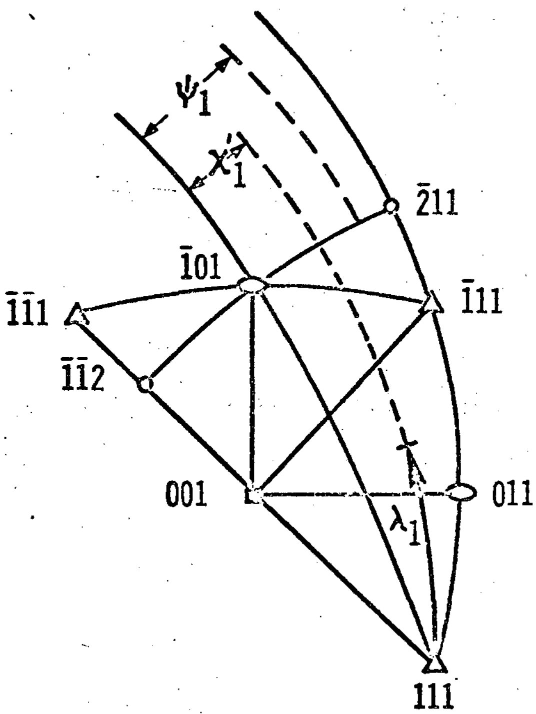

Fig. 1. Standard stereographic triangle. Symbol + represents the specimen axis. The schmid angle for slip in the [111] direction is λ_1. The angles ψ_1 and χ_1' represent the angular rotations of the observed slip plane and the plane of maximum resolved shear stress respectively from the $(\bar{1}01)$ plane.

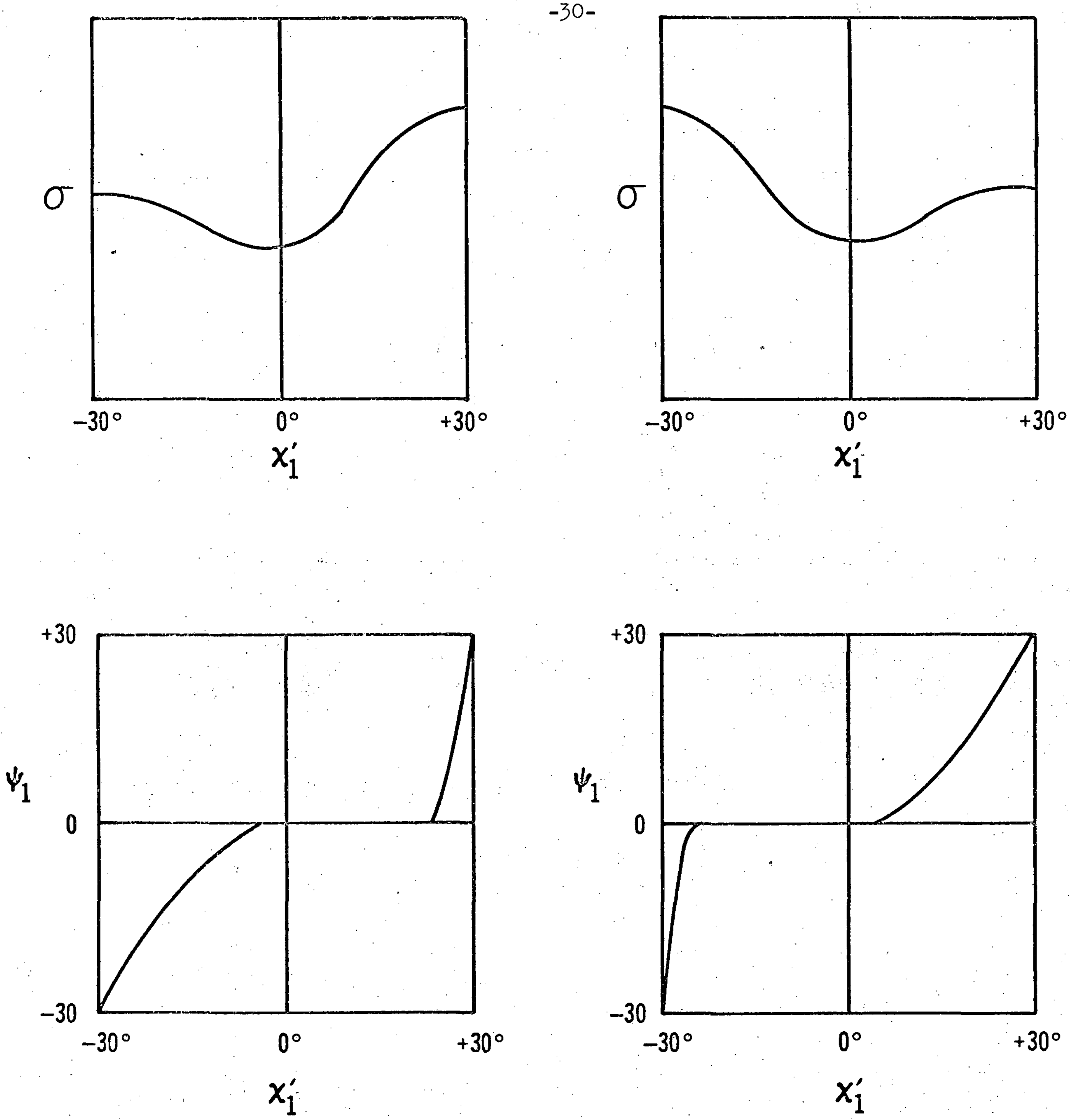

(a) TENSION (b) COMPRESSION

Fig. 2. Schematic representation of asymmetric behavior.

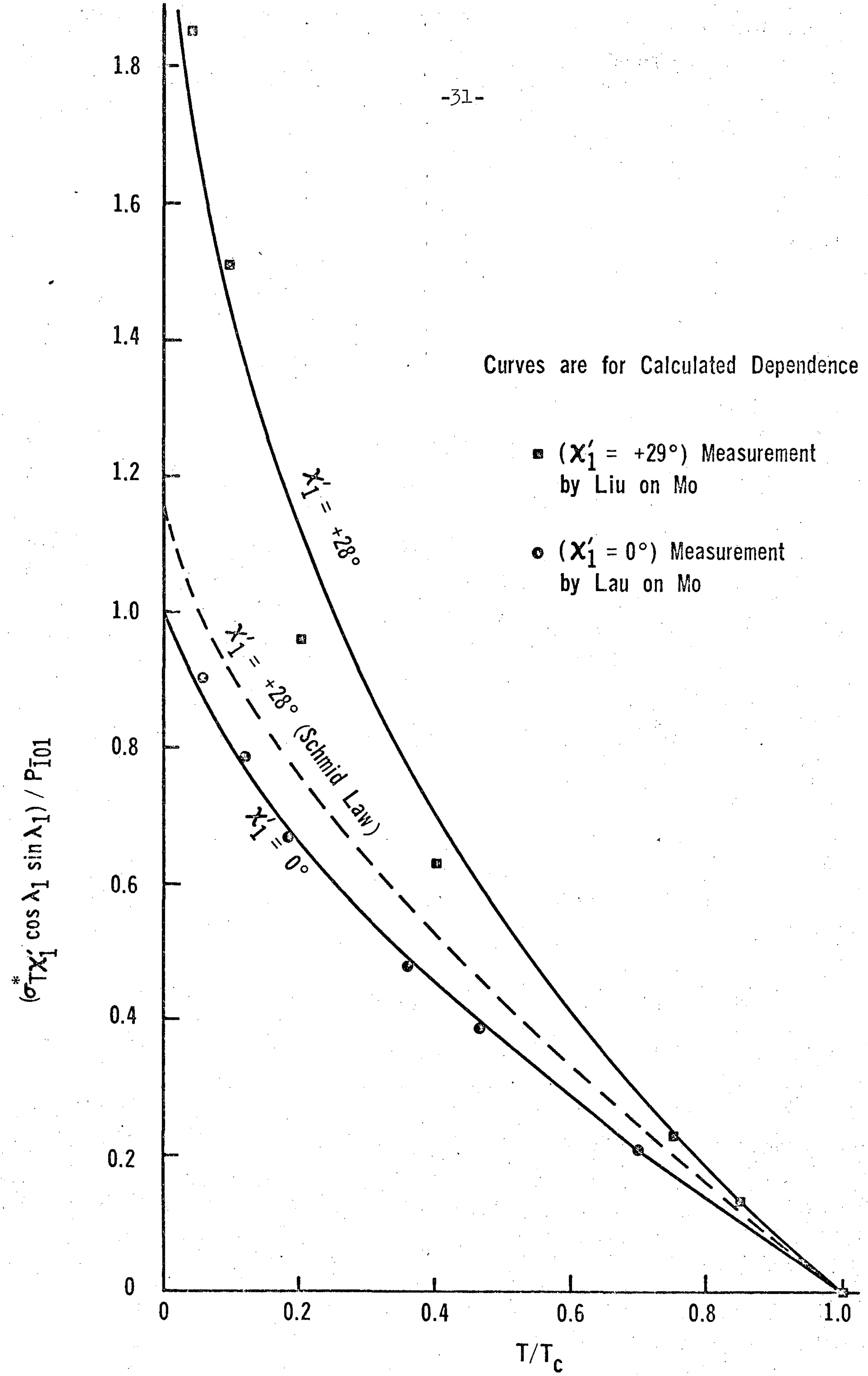

Fig. 3. Effect of asymmetry on the σ^* T relationship for Mo.

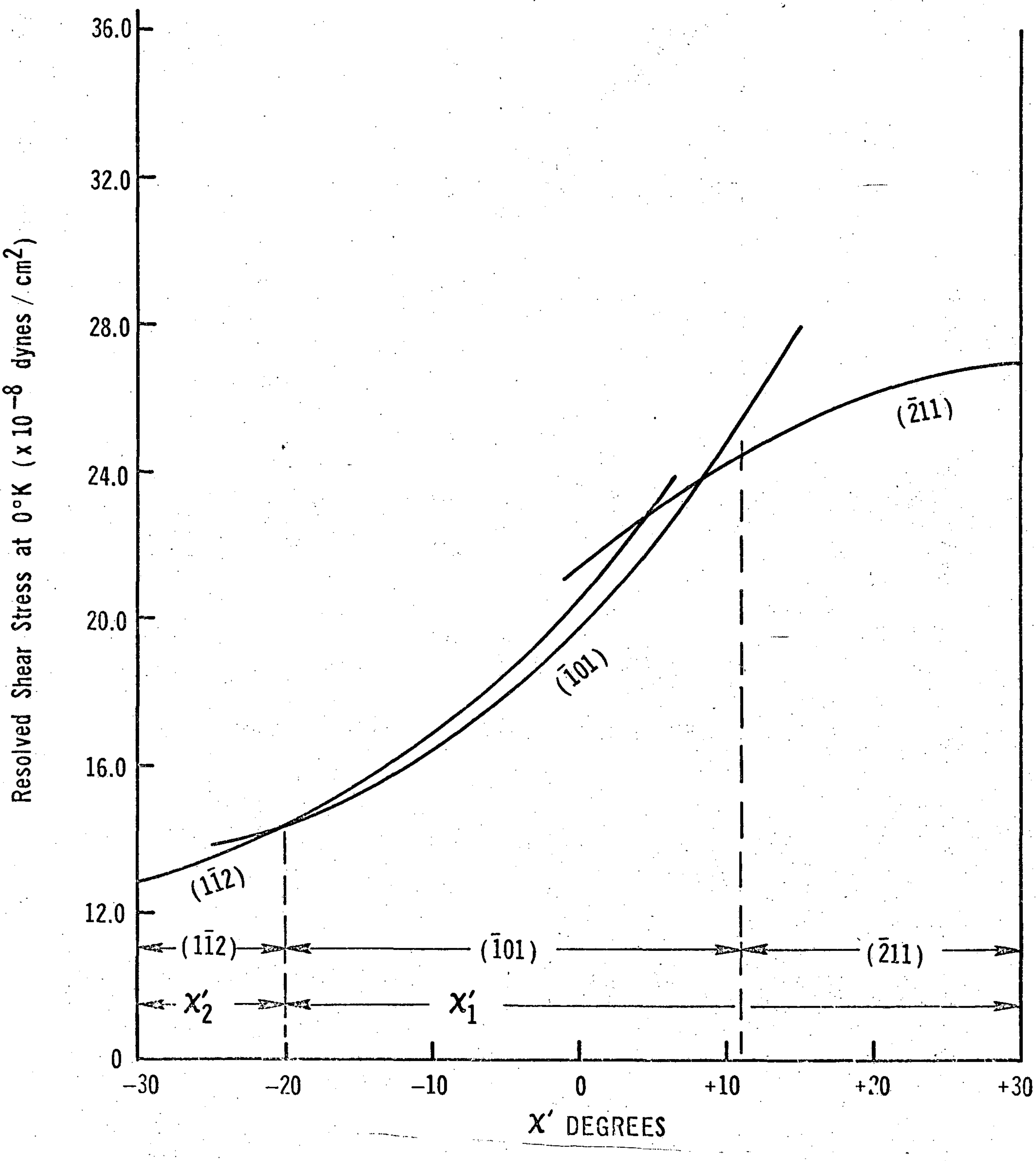

Fig. 4. Critical resolved shear stress as a function of χ' at absolute zero.

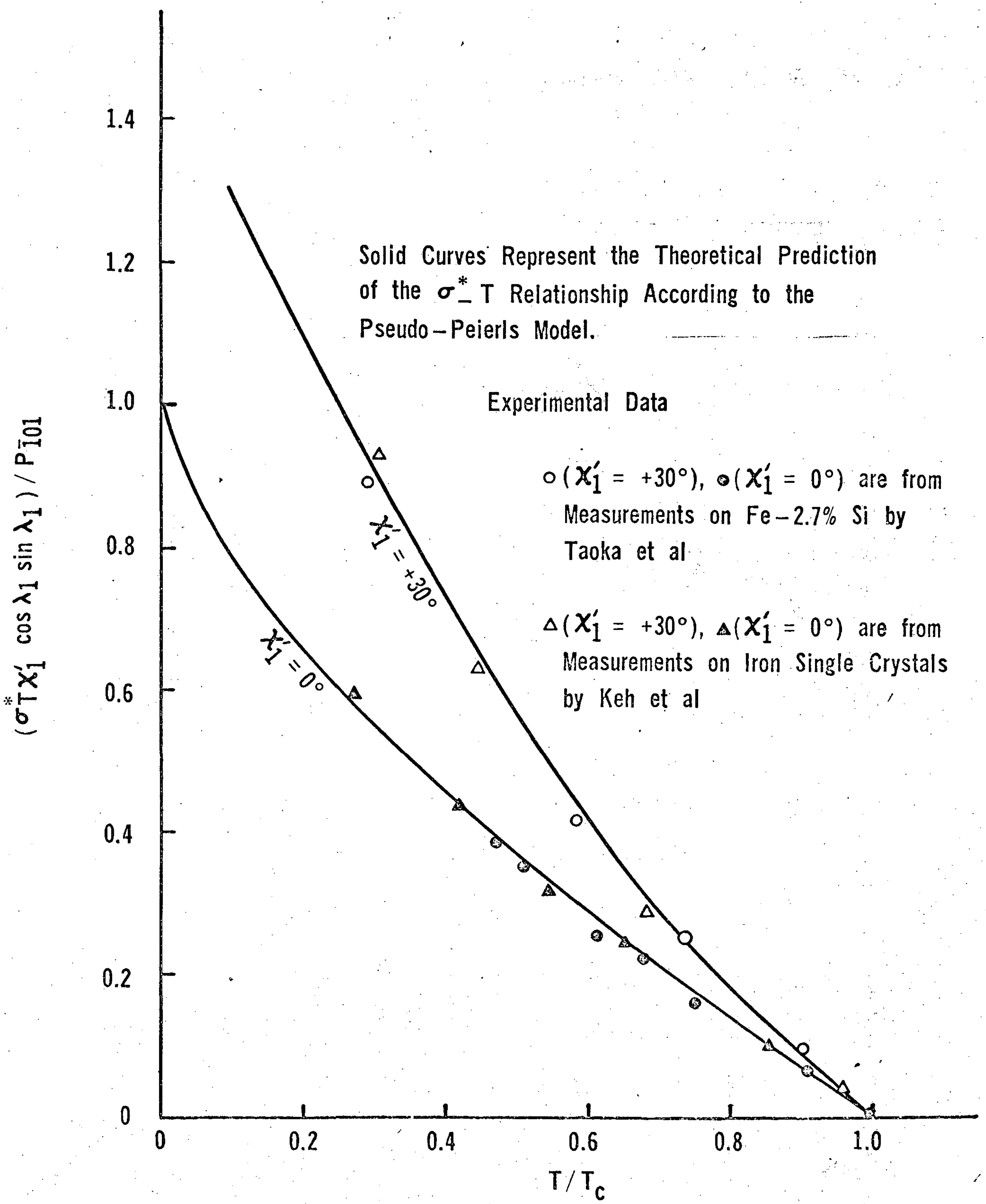

Fig. 5. Effect of asymmetry on the σ^*_- T relationship for silicon-iron and iron.

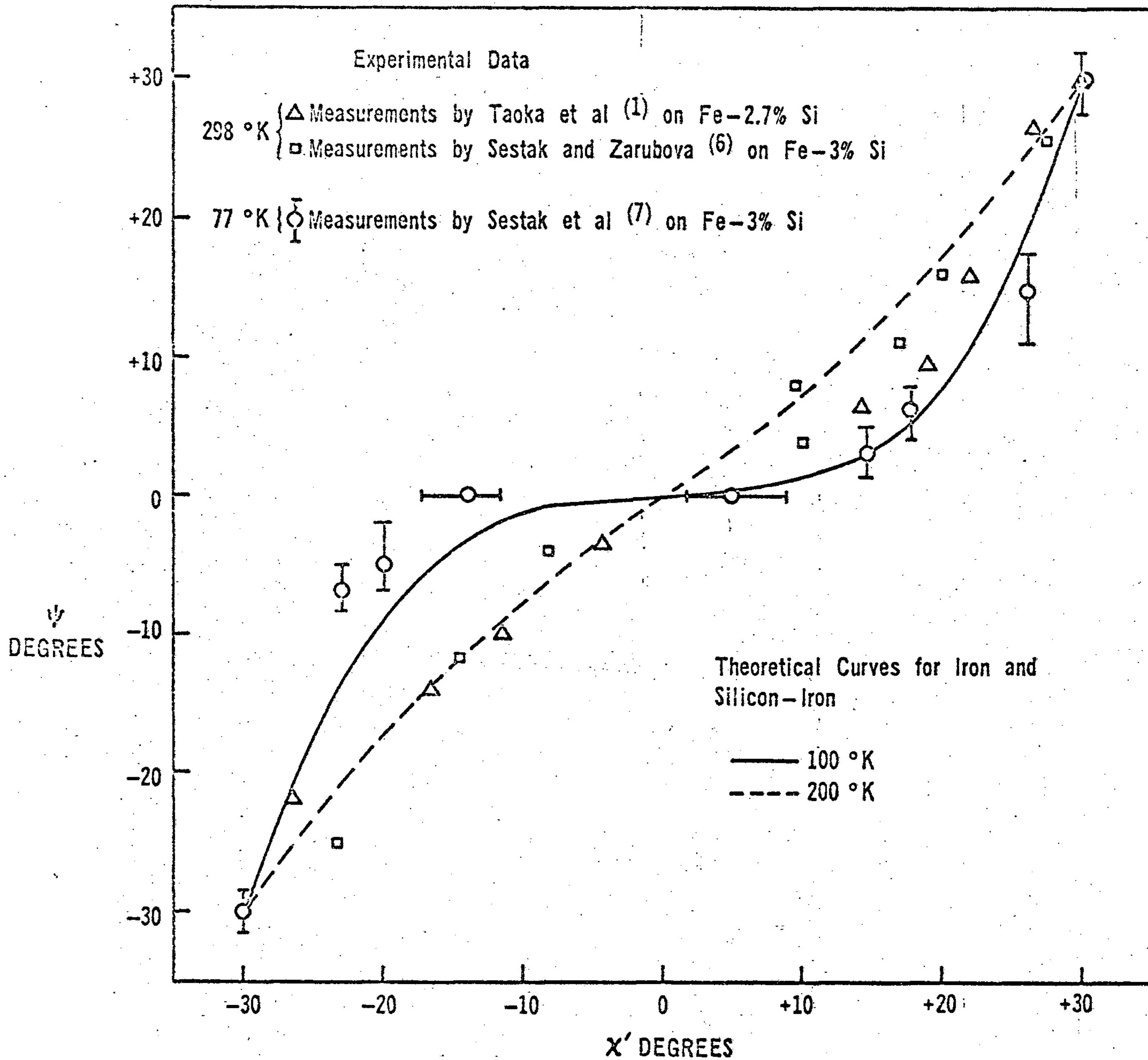

Fig. 6. Dependence of ψ on χ'

TECHNICAL INFORMATION DIVISION
LAWRENCE RADIATION LABORATORY
UNIVERSITY OF CALIFORNIA
BERKELEY, CALIFORNIA 94720